PROTOCOL FOR HEAVY DUTY HYDROGEN REFUELING: A MODELING BENCHMARK

Charolais, A.[1], Ammouri, F.[1] , Vyazmina, E.[1], Nouvelot, Q.[2], Guewouo, T.[2], Greisel, M.[3], Gebhard, M.[3], Kuroki, T.[4] and Mathison, S.[5]
[1] Air Liquide, R&D, 78350, Jouy-en-Josas, France
[2] Engie Lab CRIGEN, 93240, Stains, France
[3] Wenger Engineering, 89077, Ulm, Germany
[4] National Renewable Energy Laboratory, Golden, CO 80401, United States
[5] Shell, United States

ABSTRACT

For the successful deployment of the Heavy Duty (HD) hydrogen vehicles, an associated infrastructure, in particular hydrogen refueling stations (HRS) should be reliable, compliant with regulations and optimized to reduce the related costs. FCH JU project PRHYDE aims to develop a sophisticated protocol dedicated to HD applications. The target of the project is to develop protocol and recommendations for an efficient refueling of 350, 500 and 700 bar HD tanks of types III and IV. This protocol is based on modeling results as well as experimental data. Different partners of the PRHYDE European project are closely working together on this target. However, modeling approaches and corresponding tools must first be compared and validated to ensure the high level of reliability for the modeling results. The current paper presents the benchmark performed in the frame of the project by Air Liquide, Engie, Wenger Engineering and NREL. The different models used were compared and calibrated to the configurations proposed by the PRHYDE project. In addition, several scenarios were investigated to explore different cases with high ambient temperatures.

INTRODUCTION

Global transport greenhouse gases emissions account for over one fifth of global emissions [1]. As these emissions should be brought down to near zero in the span of a few decades, the internal combustion engine, responsible for the bulk of the emissions, should be phased out. To fulfill the indispensable need for transportation, of both people and goods, two main technologies are emerging: the battery-powered and the hydrogen-powered vehicle. As battery technology looks set to overtake light duty and passenger transport, heavy duty, including trucks, buses and trains, can benefit from using hydrogen as fuel. Therefore, development of the refueling infrastructure and associated protocols to accommodate for the planned increase in vehicle number is critical.

In particular, hydrogen refueling stations (HRS) are needed to be safe, easy-to-use and fast. The PRHYDE project [2] aims at providing insights into the future development of heavy duty vehicle refueling protocols. Such a protocol, similar to the one developed by the SAE, referenced J2601 [3], details process control requirements for the station to respect limits on gas or tank wall temperature, and gas density. Over-heating (exceeding gas or wall temperature limits) or over-filling (exceeding density limit) can lead to tank degradation over time or even a one-time failure: both should be avoided. In practice, these parameters are controlled through the gas delivery temperature, as well as the total filling time and have an outsized impact on the process cost and reliability. Hence modeling as precisely as possible the temperature and the gas density increase inside the tank is critical to achieve the best operational conditions.

Nowadays, HRS's design is based on the protocol used. Protocol development is a long and complicated process to be followed, which requires modeling tools and experimental validation. This can take up to 3 or 4 years, as in the HyTransfert project [4], which also makes the development of a standard protocol very expensive. The usage of validated modeling tools can significantly accelerate the protocol development and also reduce its cost by the diminishing of the experimental campaign. In the next 5 to 10 years, it is foreseen to replace experimental investigation by fully modeling approach. To achieve this target only validated models should be used. The current paper is dedicated to a code

benchmark performed in the frame of the PRHYDE project. It aims to compare four codes for modeling of tanks refueling, used for protocol development: SOFIL by Air Liquide, Hyfill by Engie, H2FillS by NREL and H2-Fill by Wenger. A benchmark, comparing software between them, is different from a validation, comparing a software against experimental data. Some of the software presented in this paper have already been validated previously for light duty refueling. In the PRHYDE project, experimental data will be used to validate the models in the context of heavy duty refueling later on.

Several models have already been developed and detailed. Johnson et al. [5], Galassi et al. [6], Bourgeois et al. [7], Melideo and Baraldi [8] and Melideo et al. [9] compared experimental data with CFD computations and predictions from one-dimensional modeling for hydrogen fast fillings. Average gas properties could be predicted reasonably well with simple models, and CFD computations allowed to understand more thoroughly all underlying phenomena.

PRESENTATION OF EACH SOFTWARE

Four organizations linked to the PRHYDE project have independently developed software to model the increase in temperature and pressure occurring in hydrogen tanks during their refueling. Each software solves the underlying equations in the manner detailed below.

Air Liquide's SOFIL

The SOFIL model assumes homogeneous gas temperature and pressure in the tank, and linear evolution of the tank wall. The 0D-gas/1D-wall approach has been found in comparison to experiments to be predictive, allowing to estimate the gas as well as the tank wall temperature accurately [7, 10].

The model solves mass and energy balance equations to estimate gas temperature and pressure. A real gas equation is used to obtain gas properties. The model takes into account, if present, the tank bosses. The piping, from dispenser to FCV tank, can be modelled through a lumped thermal mass or a more precise 2D (radially and longitudinally) discretization.

The pressure drop formula used to determine the mass flow into the tank is presented in Equation (1) for the sonic conditions ($P_1 > 2\ P_2$) and Equation (2) for the subsonic conditions ($P_1 \leqslant 2\ P_2$):

$$\frac{dm_g}{dt} = C\ k_v P_1 \sqrt{\frac{\rho_N}{T_1}} \tag{1}$$

$$\frac{dm_g}{dt} = 2\ C\ k_v \sqrt{\frac{\rho_N\ (P_1 - P_2) P_2}{T_1}} \tag{2}$$

where m_g is the mass of gas in the tank (kg), a constant C equal to 257, k_v the flow coefficient (m^3/h), P_1 the upstream pressure (bara) at the dispenser, P_2 the downstream pressure (bara) in the tank, ρ_N the gas density at normal conditions 0°C, 1 atm (kg/Nm^3) and T_1 the upstream temperature (K).

Engie's Hyfill

In order to contribute to the reflection on hydrogen mobility and more particularly on hydrogen refueling stations, the Engie Lab CRIGEN has initiated the development of a tool called HyFill. HyFill developed on Matlab/Simulink allows to simulate the fast filling and emptying of hydrogen tanks in order to predict the final temperature reached by the hydrogen. HyFill is a pseudo-1D model. It considers that the gas temperature is uniform at each instant in the tank. The heat transfer between the gas and the outside is modeled by the unsteady 1D cylindrical conduction equation.

To have access to the temperature, mass and pressure of the gas in the tank, a system of three equations is solved at each time step during the whole filling or emptying simulation; these are the mass rate balance, the energy rate balance for a control volume and the equation of state here given by [11]:

$$\begin{cases} \frac{dm}{dt} = \dot{m}_{in} - \dot{m}_{out} \\ \frac{dmu}{dt} = \dot{m}_{in} h_{in} - \dot{m}_{out} h_{out} - Q_{gas-wall} \\ \frac{P}{\rho} = ZRT \end{cases} \quad (3)$$

In this equation system, m is the hydrogen mass in the tank, $\dot{m}_{in}$ and $\dot{m}_{out}$ are the inlet and outlet mass flow rate respectively, u is the specific internal energy, h is the specific enthalpy, P, T and ρ are hydrogen pressure, temperature and density respectively, Z is the hydrogen compressibility factor, R is the gas constant. The hydrogen compressibility factor as well as all other thermodynamic properties of hydrogen are calculated in HyFill using the GERG-2008 equation of state. It is valid for various gas and gas mixture, for pressures from 0 to 3000 bar and temperatures from 77 to 473K, thus covering a wide range of permissible temperatures and pressures when filling or emptying a tank with various gases. The GERG-2008 equation of state defines the thermodynamic properties as explicit functions of the Helmholtz free energy. For a given gas or gas mixture, the Helmholtz free energy depends on the reduced temperature $\tau = \frac{T_c}{T}$, reduced density $\delta = \frac{\rho}{\rho_c}$ and mole fractions x of the different components of the gas mixture (where T_c and P_c are the critical temperature and critical density of the gas or gas mixture, respectively). Equations for thermodynamic properties as a function of Helmholtz free energy are given in Table B1 of reference [12].

$Q_{gas-wall}$ is the heat flow from gas to the inner tank wall given by:

$$Q_{gas-wall} = S_{in} H_{in} \left(T - T_{wall_{r=r_{in}}} \right) \quad (4)$$

Where S_{in} is the inner wall surface of the tank, H_{in} is the inner film heat transfer coefficient determined from the correlation for internal turbulent flow [13], $T_{wall_{r=r_{in}}}$ is the temperature of the inner wall of the tank. It is obtained by solving the unsteady one-dimensional radial heat conduction equation (assuming azimuthal symmetry as the tank wall temperature is the same along its entire length for a given radius) given by [14], in Equation (5):

$$\rho c_p \frac{\partial T}{\partial t} = \frac{\lambda}{r} \frac{\partial}{\partial r} \left(r \frac{\partial T}{\partial r} \right) . \quad (5)$$

The boundary conditions necessary to solve this equation being the heat flow from gas to the inner tank wall ($Q_{gas-wall}$) and the heat flow from the outer tank wall to the ambient air:

$$Q_{wall-air} = S_{out} H_{out} \left(T_{wall_{r=r_{out}}} - T_{amb} \right) + \varepsilon_{wall} \sigma S_{out} (T^4_{wall_{r=r_{out}}} - T^4_{amb}) \quad (6)$$

where H_{out} is the outer film heat transfer coefficient kept constant (natural convection assumption), S_{out} is the outer wall surface of the tank, $T_{wall_{r=r_{out}}}$ is the temperature of the outer wall of the tank, T_{amb} is the ambient temperature, ε_{wall} is the emissivity of the external wall of the tank, σ is the Stefan-Boltzmann constant.

The pressure drop formula used to determine the mass flow into the tank is presented in Equation (7) for the sonic conditions ($P_1 > 2\ P_2$) and Equation (8) for the subsonic conditions ($P_1 \leqslant 2\ P_2$):

$$\frac{dm_g}{dt} = \rho_1\ N\ k_v\ Y \sqrt{\frac{P_1}{2\rho_1}} \text{ with } Y = \frac{2}{3} \quad (7)$$

$$\frac{dm_g}{dt} = \rho_1 \, N \, k_v \, Y \sqrt{\frac{(P_1 - P_2)}{\rho_1}} \text{ with } Y = 1 - \frac{2}{3}\frac{P_1 - P_2}{P_1} \quad (8)$$

where mg is the mass of gas in the tank (kg), ρ1 the upstream gas density (kg/m³), N a constant equal to 31.6, kv the flow coefficient (m³/h), P1 the upstream gas pressure (bara) at the dispenser, P2 the downstream gas pressure (bara) in the tank and Y an adimensional term depending on the pressure levels P1 and P2.

NREL's H2FillS

The tank model described in [15, 16] has been implemented in the H2FillS software.

Initially, the FCEV tank is given a pressure, temperature, internal volume, internal surface area, internal diameter, and the thermal properties of the liner and carbon fiber reinforced polymer (CFRP). After the values are set to the tank model, the mass and energy balances are calculated with the assumption that the tank volume does not increase with the pressure rise. The governing equations for the mass and energy balances are shown as follows:

$$\frac{d}{dt}(m) = \dot{m}_{in} \quad (9)$$

$$\frac{d}{dt}(mu) = \dot{m}_{in} h_{in} + A_{wall} \alpha_{in} (T_{wall}|_{x=0} - T) \quad (10)$$

where m is the hydrogen mass, u is the specific internal energy, m_{in} is the mass flow rate, h_{in} is the specific enthalpy, A_{wall} is the inner surface area in the tank, a_{in} is the heat transfer coefficient at the inner surface, T is the hydrogen temperature, $T_{wall}|_{x=0}$ is the inner surface wall temperature, dt is the time step, and t is the time. When the energy and mass balances are solved by the equations, the state inside the tank is assumed to be a lumped model; thus, the acquired temperature and pressure are treated as mean values calculated by the bulk specific internal energy and density. The heat conduction in the wall is assumed to be one-dimensional. It is assumed that the tank wall is a flat plate, even though the tank shape is cylindrical. This is because the curvature radius of the tank is large compared to the wall thickness. (The effectiveness of this assumption has been examined.) Hence, the following unsteady heat conduction equation and boundary conditions are applied to obtain the temperature distribution in the wall:

$$\frac{\partial T_{wall}}{\partial t} = a_{wall} \frac{\partial^2 T_{wall}}{\partial x^2} \quad (11)$$

$$-\lambda_{wall} \frac{\partial T_{wall}}{\partial x}\Big|_{x=0} = \alpha_{in} (T - T_{wall}|_{x=0}) \quad (12)$$

$$-\lambda_{wall} \frac{\partial T_{wall}}{\partial x}\Big|_{x=l} = \alpha_{out} (T_{wall}|_{x=l} - T_{amb}) \quad (13)$$

where a_{wall} is the thermal diffusivity, x is the position at which $x = 0$ is the inner wall surface and $x = l$ is the total thickness of the wall, λ_{wall} is the thermal conductivity, a_{out} is the heat transfer coefficient at the outer surface, and T_{amb} is the ambient temperature. The value of a_{out} was set to 8.0 W/(K·m²). The value of a_{in} was derived from a Nusselt number correlation based on the Reynolds number at the tank inlet and Rayleigh number inside the tank.

The equations implemented in the model for the mass flow calculation are based on two steps:

1. Volumetric flow rate (m³/h) calculation: calculates the volumetric flow rate based on the differential pressure at the inlet and outlet of the valve ($P_{upstream}$ and $P_{downstream}$), temperature at the inlet of the valve $T_{upstream}$, and specific gravity to air G.
   If $P_{upstream} \geq 0.5 * P_{downstream}$ (non-choked flow):

$$\dot{V} = 2930\, C_v \sqrt{\frac{(P_{upstream} - P_{downstream})(P_{upstream} + P_{downstream})}{P_{upstream} GT_{upstream}}} \quad (14)$$

If $P_{upstream} < 0.5 * P_{downstream}$ (choked flow):

$$\dot{V} = 2538 C_v \frac{P_{upstream}}{GT_{upstream}} \quad (15)$$

2. Conversion to mass flow rate (kg/s): Converts the volumetric flow rate (m^3/h) to the mass flow rate (kg/s) using density at 0.1 MPa and 15.6 °C and a coefficient β, developed to handle the unsteady flow during the fueling process:

$$\dot{m} = \frac{\beta \rho \dot{V}}{3600} \quad (16)$$

Wenger's H2-Fill

H2-Fill calculates gas pressure and temperature curves in a vehicle tank for refueling and defueling with gaseous hydrogen.

An individual vehicle tank system size, configuration and type can be used for simulation with H2-Fill. The tank starts with initial conditions for gas pressure (Initial gas pressure) and gas respectively vessel wall temperature (Initial tank temperature).

The fuel gas is delivered by the station with a given pressure and a given fuel temperature (Precooling temperature). For fueling simulation, the station either ramps up pressure with a linear rate (Ramp rate) starting from the initial tank pressure and using a fixed standard pressure drop coefficient to derive a certain mass flow or directly uses a prescribed constant mass flow (Mass flow).

Heat transfer to ambience from idealized station and car components including vessel depends on ambient temperature (Ambient temperature). Fuel from the station exchanges heat with the thermal masses constituted by the fueling hose, pipes, and vehicle line components. Each thermal mass is characterized by its mass, specific heat capacity, and thermal conductivity. They exchange heat with the environment at ambient temperature.

The fuel gas enters the tank vessel and mass and energy balance are solved in order to obtain the gas temperature and pressure curves over time. It is assumed that the gas inside the tank is always perfectly mixed.

All properties of the gas inside the vessel are computed from the gas equation of state. The heat transfer rate between gas and vessel internal surface (liner) is calculated from a set of Nusselt equations for various geometries and for forced and free convection. The vessel wall is discretized in radial direction and the transient heat conduction equation is solved in one dimension. This yields the temperature profile inside the vessel. On the outer surface, the vessel wall exchanges heat with the environment, the heat transfer coefficient is again based on a set of Nusselt equations for various geometries and for free convection.

MODELLED CASES

Three cases will be modelled, for each pressure class: H35 (up to 35 MPa), H50 (up to 50 MPa) and H70 (up to 70 MPa). In each case, four 350 L type IV tanks will be filled in 10 minutes, with a constant pressure ramp rate. The tanks characteristics are detailed in Table 1, and the bosses characteristics are detailed in Table 2.

Table 1. Characteristics of the modelled tanks.

Description	H35	H50	H70	Unit
Internal volume	0.350	0.350	0.350	m^3
Internal length	1.240	1.240	1.240	m

Internal radius	0.300	0.300	0.300	m
Liner thickness	0.005	0.005	0.005	m
Liner material density	945	945	945	$kg.m^{-3}$
Liner material specific heat capacity	2100	2100	2100	$J.kg^{-1}.K^{-1}$
Liner material thermal conductivity	0.38	0.38	0.38	$W.m^{-1}.K^{-1}$
Liner mass	13.88	13.88	13.88	kg
Composite thickness	0.015	0.022	0.032	m
Composite material density	1494	1494	1494	$kg.m^{-3}$
Composite material specific heat capacity	1120	1120	1120	$J.kg^{-1}.K^{-1}$
Composite material thermal conductivity	0.5	0.5	0.5	$W.m^{-1}.K^{-1}$
Composite mass	69.3	103.5	154.4	kg
Injector diameter	5.4	5.4	5.4	mm

Table 2. Bosses characteristics. Values refer to both bosses.

Description	H35 / H50 / H70	Unit
Bosses material density	7900	$kg.m^{-3}$
Bosses material specific heat capacity	500	$J.kg^{-1}.K^{-1}$
Bosses volume	0.002	$W.m^{-1}.K^{-1}$
Bosses contact surface with hydrogen	0.045	m^2
Bosses contact surface with ambient air	0.047	m^2
Bosses mass	15.8	kg

The filling parameters for each pressure class are detailed in Table 3. They were chosen to simulate average fills. The goal of these simulations is to compare the software's results.

Table 3. Filling parameters for each pressure class.

Description	H35	H50	H70	Unit
Initial pressure (tank and dispenser)	60	80	100	barg
End dispenser pressure (1.25 NWP)	437.5	625	875	barg
Ambient temperature	15	15	15	°C
Constant dispenser temperature	15	5	-10	°C
Initial gas temperature	15	15	15	°C
Filling time	10	10	10	min
Corresponding APRR*	0.629167	0.90833	1.29167	bar/s
Corresponding APRR*	3.775	5.45	7.75	MPa/min

APRR: Average Pressure Ramp Rate

The pressure drop is computed with the values referenced in Table 4. The values chosen represent the actual pressure drop from an H35 bus refueling. For the H50 and H70 cases, actual data is non-existent at the moment. Therefore, the pressure drop was adapted by changing the reference mass flow, computed by taking the total CHSS (Compressed Hydrogen Storage System) times 1.5 divided by the filling time.

Table 4. Pressure drop reference values for each pressure class.

Description	H35	H50	H70	Unit
Reference pressure	100	100	100	barg
Reference pressure drop	72.19	72.19	72.19	bar
Reference dispenser pressure	172.19	172.19	172.19	barg
Reference dispenser temperature	-15	-15	-15	°C

Reference mass flow	84.1734	110.9048	140.7492	g/s

No heat exchange in the piping (between the dispenser and the tank) is taken into account.

RESULTS OF THE COMPARISON

In this section, the three cases have been run with each software. The differing results are then analyzed.

H35 simulations

Without pre-cooling the gas, with the ambient temperature of 15°C, the H35 filling sees the gas temperature increase from 15 °C to about 81 °C. As shown in Fig. 1, predictions at the end-of-fill differ by less than 2 °C. Table 5 summarizes the end-of-fill parameters for the H35 filling, given by each software.

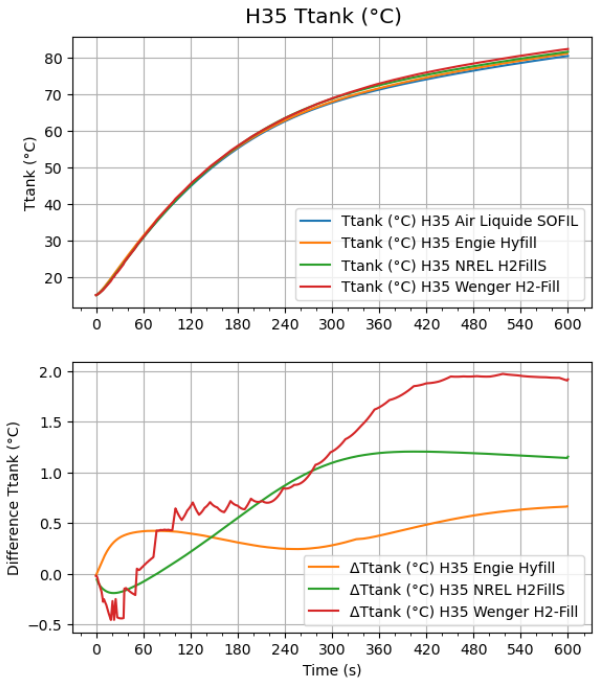

Figure 1. Tank gas temperature evolution (above) and difference with Air Liquide's SOFIL (below) during the H35 filling.

Figs. 2a and 2b show the evolution of the tank gas pressure and SOC respectively. Again, the models all seem to be in accordance, with the predicted end-of-fill pressure differing by less than 0.45 MPa and the SOC by less than 1.3 %. These differences are coherent: the model predicting the lowest gas pressure, Wenger's H2-Fill, also predict the lowest SOC.

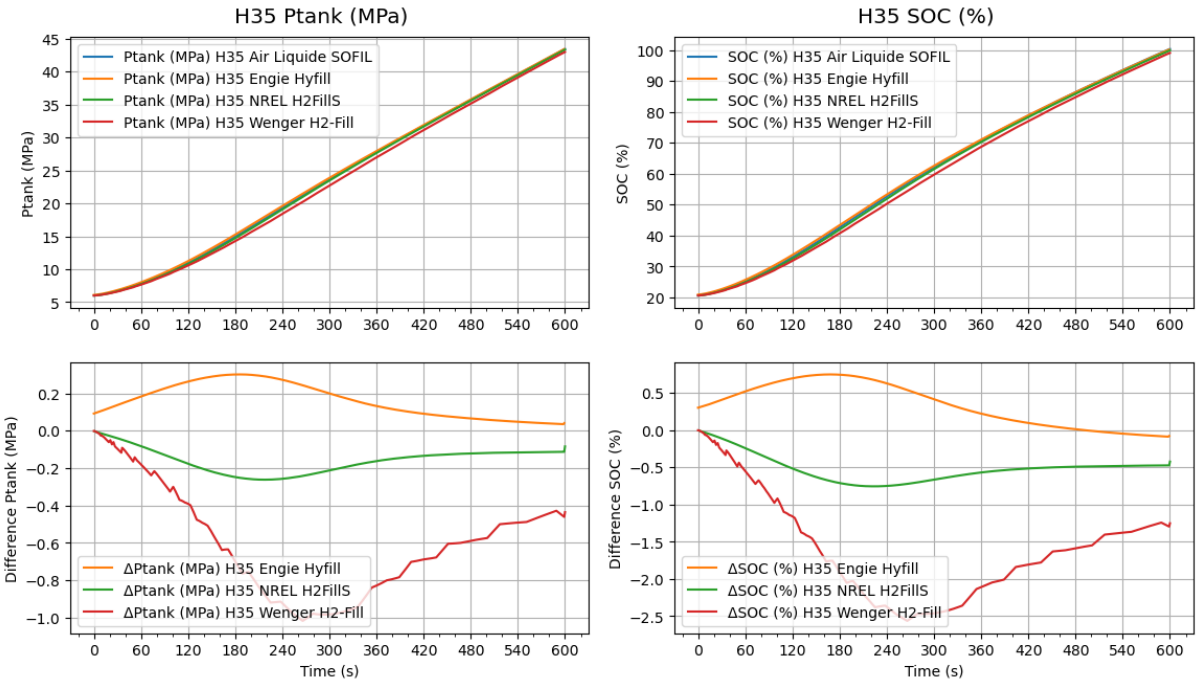

Figure 2. (a) Left. Tank gas pressure evolution (above) and difference with Air Liquide's SOFIL (below) during the H35 filling. (b) Right. Tank gas SOC evolution (above) and difference with Air Liquide's SOFIL (below) during the H35 filling.

Wenger's H2-Fill also predicts the highest gas temperature. As shown in Fig. 3, the simulated mass flow is, relative to the other three models, lower until about 260 seconds, and higher after this point. The total mass entering the tank may therefore be different, explaining the lower SOC.

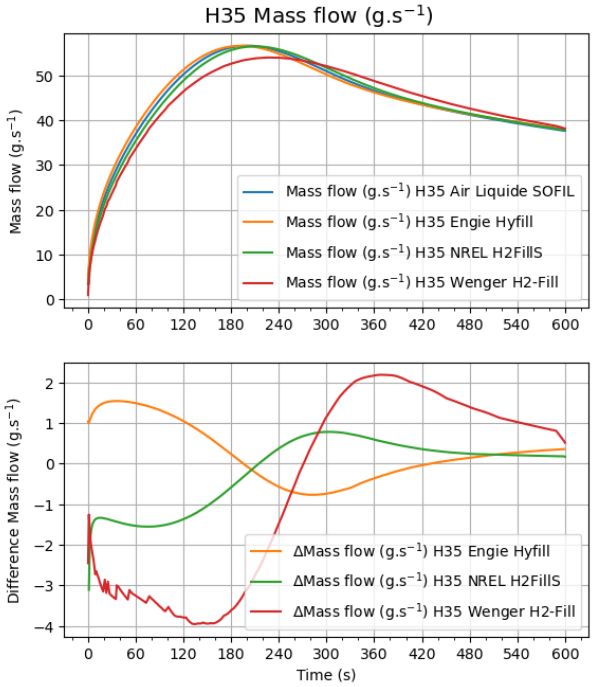

Figure 3. Mass flow into the tank evolution (above) and difference with Air Liquide's SOFIL (below) during the H35 filling.

The higher end-of-fill temperature in Wenger's H2-Fill model may be due to the higher mass flow than that of the other models towards the end of the filling. The increase in gas temperature is therefore higher at the end of the filling, allowing less time for heat dissipation.

This dependency on the timing of the increase in temperature is also visible, by analyzing Engie's Hyfill and NREL's H2FillS relative predictions in gas temperature and mass flow. It seems that, for the simulated 10-minutes fillings, a higher mass flow at the beginning of the fill results in a lower end-of-fill gas temperature prediction.

Table 5. End-of-fill values predicted by each software for the H35 filling.

H35	Ttank (°C)	Ptank (MPa)	Mass flow ($g.s^{-1}$)	SOC (%)
Air Liquide SOFIL	80.5	43.4	37.6	100.3
Engie Hyfill	81.1	43.4	38.0	100.2
NREL H2FillS	81.6	43.3	37.8	99.9
Wenger H2-Fill	82.4	43.0	38.1	99.1

H50 and H70 simulations

Two additional cases were run with each software: H50 and H70. In both these cases, the global evolution of the gas in the tank is similar in each prediction. Figs. 4a and 4b show the evolution and relative difference in the gas temperatures.

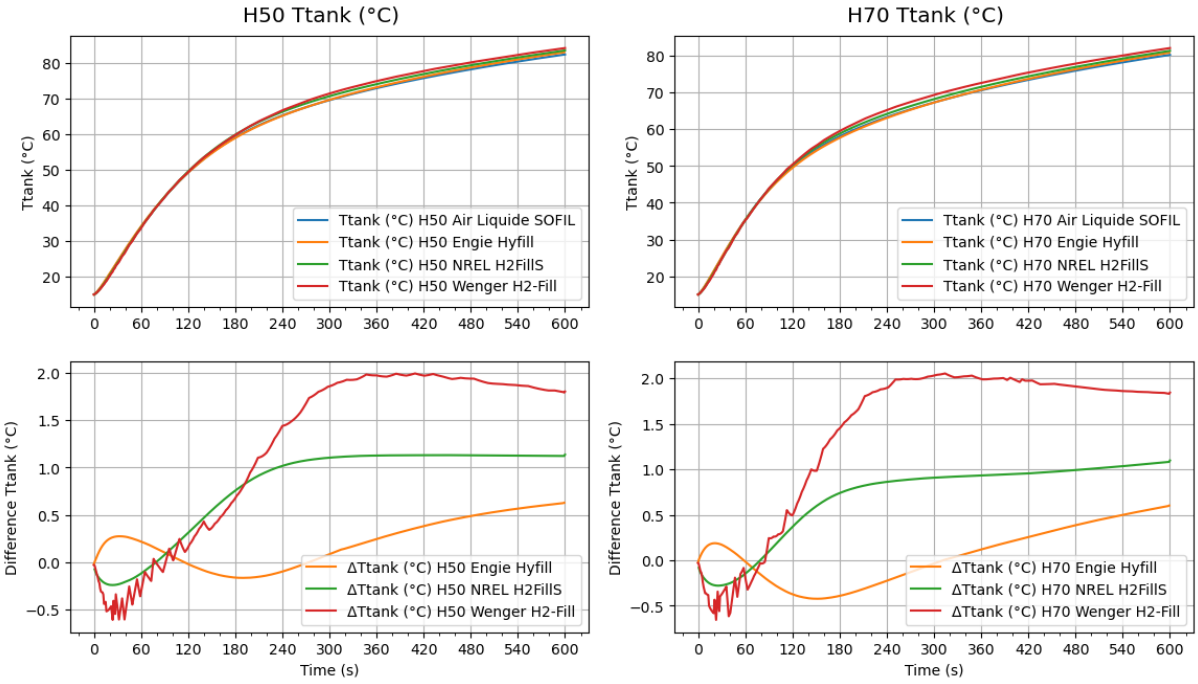

Figure 4. (a) Left. Tank gas temperature evolution (above) and difference with Air Liquide's SOFIL (below) during the H50 filling. (b) Right. Tank gas temperature evolution (above) and difference with Air Liquide's SOFIL (below) during the H70 filling.

Figs. 5a and 5b, as well as Figs. 6a and 6b, show the evolution of pressure and SOC in the H50 and H70 cases. Again, the models are coherent and predict end-of-fill values close to each other, as shown in Tables 6 and 7. Relative differences between the models are similar to the H35 case: Wenger's H2-Fill model predicts the highest temperature and the lowest pressure and SOC. The other three

predictions follow the same order as in the H35 simulations: NREL's H2FillS predicts the second highest temperature, then Engie's Hyfill and then Air Liquide's SOFIL.

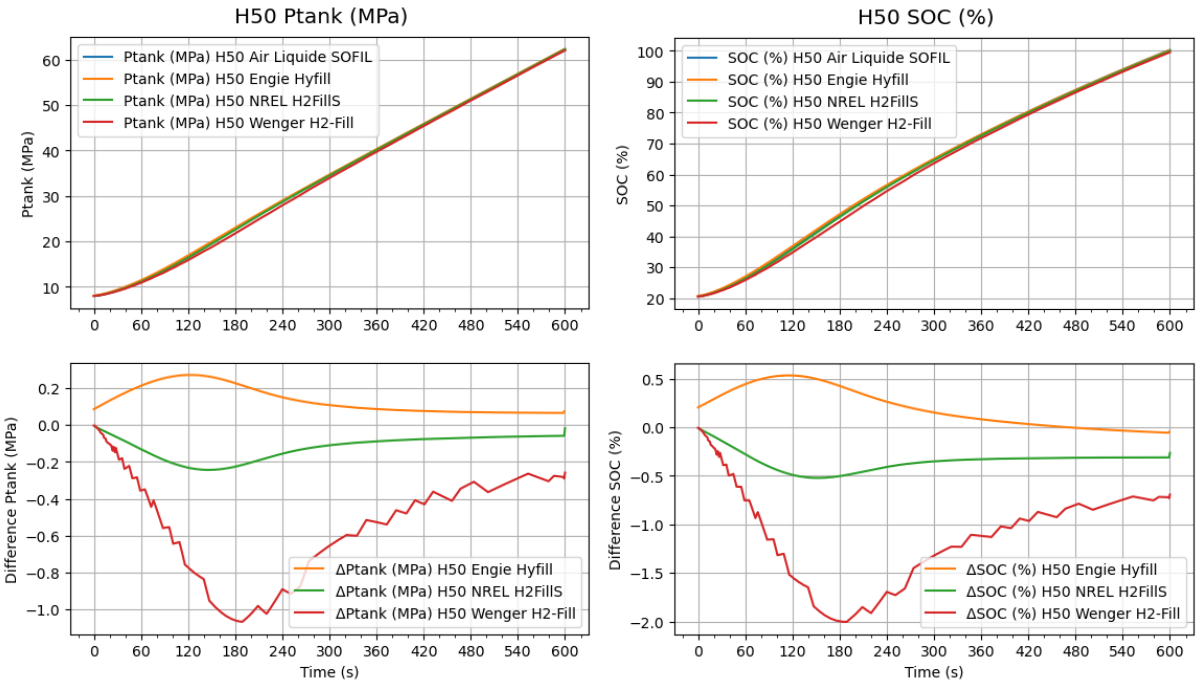

Figure 5. (a) Left. Tank gas pressure evolution (above) and difference with Air Liquide's SOFIL (below) during the H50 filling. (b) Right. Tank gas SOC evolution (above) and difference with Air Liquide's SOFIL (below) during the H50 filling.

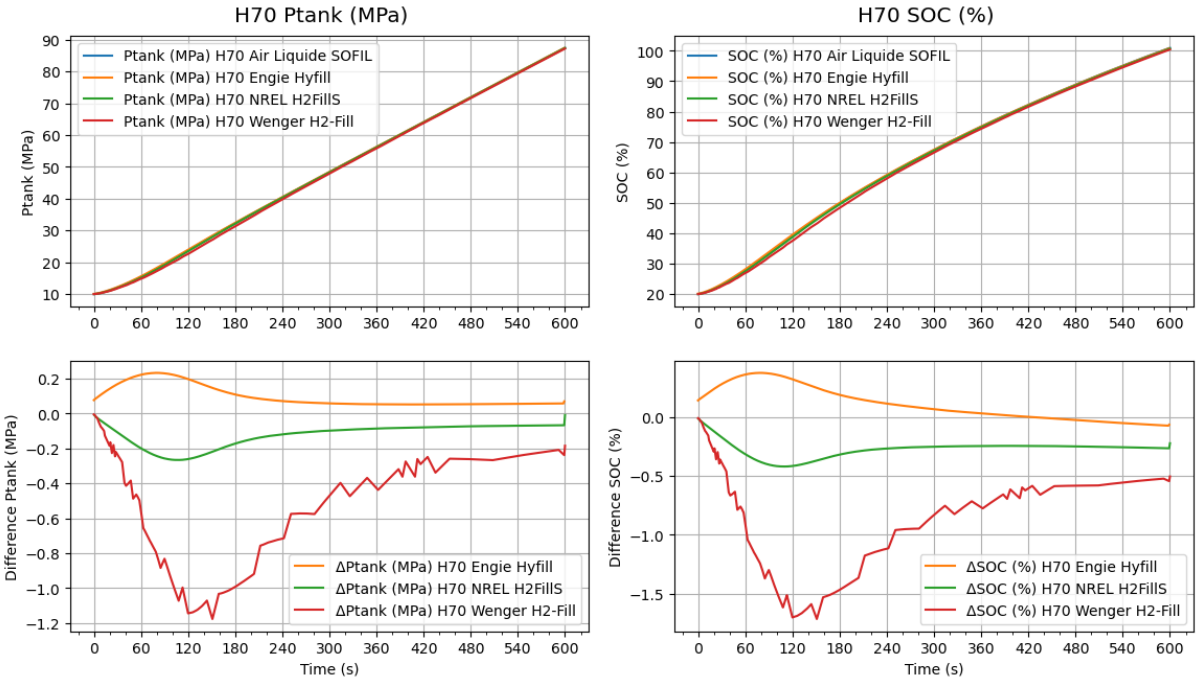

Figure 6. (a) Left. Tank gas pressure evolution (above) and difference with Air Liquide's SOFIL (below) during the H70 filling. (b) Right. Tank gas SOC evolution (above) and difference with Air Liquide's SOFIL (below) during the H70 filling.

Lastly, the mass flow predictions by each model, for the H50 and H70 cases, have a similar relative evolution to each other, as shown in Figs. 7a and 7b.

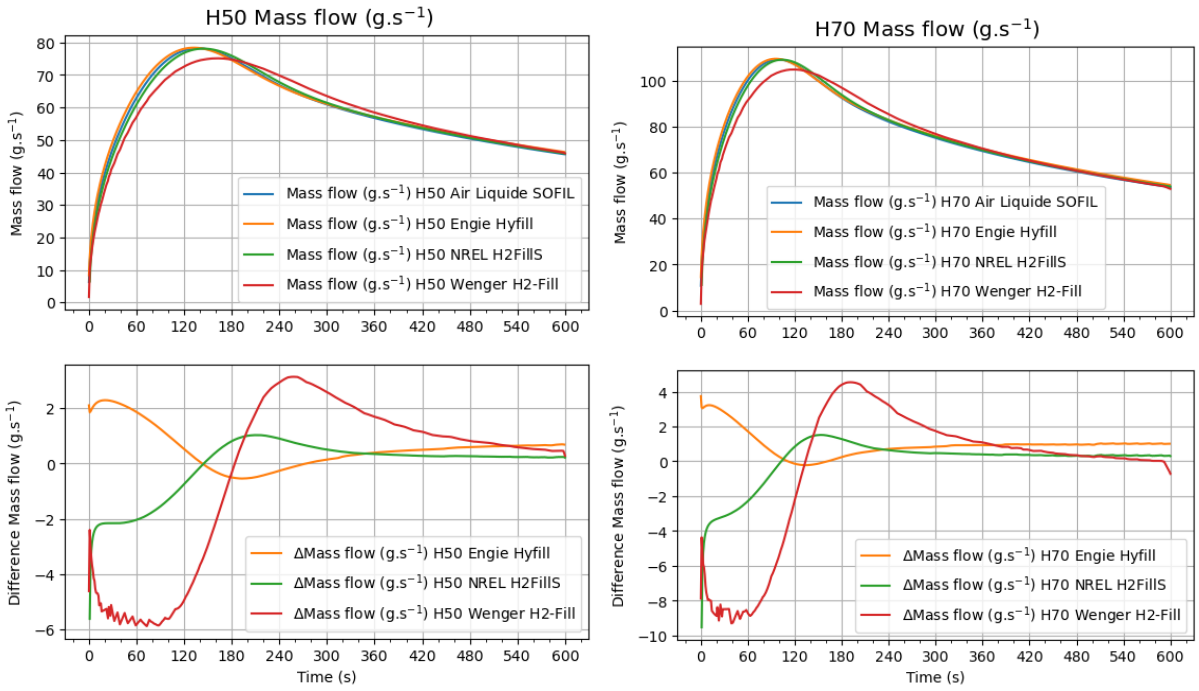

Figure 7. (a) Left. Mass flow into the tank evolution (above) and difference with Air Liquide's SOFIL (below) during the H50 filling. (b) Right. Mass flow into the tank evolution (above) and difference with Air Liquide's SOFIL (below) during the H70 filling.

Table 6. End-of-fill values predicted by each software for the H50 filling.

H50	Ttank (°C)	Ptank (MPa)	Mass flow (g.s^{-1})	SOC (%)
Air Liquide SOFIL	82.4	62.3	45.6	100.2
Engie Hyfill	83.0	62.3	46.3	100.1
NREL H2FillS	83.5	62.3	45.8	100.0
Wenger H2-Fill	84.2	62.0	45.9	99.5

Table 7. End-of-fill values predicted by each software for the H70 filling.

H70	Ttank (°C)	Ptank (MPa)	Mass flow (g.s^{-1})	SOC (%)
Air Liquide SOFIL	80.3	87.4	53.6	100.9
Engie Hyfill	80.8	87.4	54.7	100.8
NREL H2FillS	81.4	87.4	53.9	100.7
Wenger H2-Fill	82.1	87.2	52.9	100.4

Explaining the differences

The differences in the predictions given by the models, detailed in the previous subsections, may come from a number of differences in their implementations of the studied problem. First, the real gas equation used to compute the hydrogen properties in the tank may vary slightly. The differences in gas properties may amount to a few percent, which, over the course of the simulation, may alter the results.

Second, each model may represent the bosses in distinct ways. As these are metallic, their capacity to evacuate heat is high relative to the tank walls. Taking them into account may lead to a lower end-of-fill temperature. In fact, NREL's H2FillS model does not take the bosses into account.

Third, the implementation of the tank dimensions, length and diameter, into internal and external surfaces may vary depending on the model, as shown in Table 8. As these surfaces are directly used in the heat exchange between the gas, tank wall and ambient medium, this can affect the predictions. Another way for the distinct implementations to affect the simulations is the deduced mass of liner and composite. As the geometry of the tank is simplified in various ways by each software, this can lead to masses being slightly different from each other. As the tank walls store some of the heat produced during the filling, this also affects the end-of-fill predictions. The external boundary condition may also affect slightly the results: a constant heat exchange coefficient or natural convection correlation is used depending on the models.

Table 8. Tank geometry used in each model for the H35 case.

H35 tank	Internal surface (m^2)	External surface (m^2)	Liner mass (kg)	Composite mass (kg)
Air Liquide SOFIL	2.90	3.21	13.88	69.33
Engie Hyfill	2.76	3.02	12.96	64.38
NREL H2FillS	2.89	3.21	13.80	69.30
Wenger H2-Fill	2.90	3.21	43.98*	61.26

* In Wenger H2-Fill model, the thermal mass from both bosses was included in the liner.

Last, as the quantity of gas entering the tank influences directly the filling, the model ability to estimate the mass flow is critical. Each software implements a different simplified formula to evaluate this physical quantity, leading to variable estimations of the final gas properties.

CONCLUSION

The four models from Air Liquide, Engie, NREL and Wenger are described and compared on three benchmark cases in this paper. All models are in good general agreement. The end-of-fill properties of the gas were very similar in each prediction, with end-of-fill temperature predictions within less than a 2 °C range. This range is in accordance with the expected accuracy of the models and we could therefore deduce that all models are acceptable to the use of refueling simulations. The differences observed may be explained by the real gas equations used to compute the gas properties, the bosses presence in the models, the simplified tank geometry implemented, and the pressure drop formula leading to slightly different simulated mass flows. Additionally, these models will be confronted to experimental data on large tanks in the next steps from the PRHYDE project.

These types of model, giving a quick result on average temperature in the tank, is useful for rapid, safe and efficient protocol development, as in the PRHYDE project: the models can provide quick feedback on different approaches as well as give an estimation of the influence of each parameter.

ACKNOWLEDGEMENT

Research leading to these results is part of a project that has received funding from the Fuel Cells and Hydrogen 2 Joint Undertaking under Grant Agreement No 874997. This Joint Undertaking receives support from the European Union's Horizon 2020 Research and Innovation program, Hydrogen Europe and Hydrogen Europe Research.

REFERENCES

1. Sims R., R. Schaeffer, F. Creutzig, X. Cruz-Núñez, M. D'Agosto, D. Dimitriu, M.J. Figueroa Meza, L. Fulton, S. Kobayashi, O. Lah, A. McKinnon, P. Newman, M. Ouyang, J.J. Schauer, D. Sperling, and G. Tiwari, 2014: Transport. In: Climate Change 2014: Mitigation of Climate Change. Contribution of Working Group III to the Fifth Assessment Report of the Intergovernmental Panel on Climate Change [Edenhofer, O., R. Pichs-Madruga, Y. Sokona, E. Farahani, S. Kadner, K. Seyboth, A. Adler, I. Baum, S. Brunner, P. Eickemeier, B. Kriemann, J. Savolainen, S. Schlömer, C. von Stechow, T. Zwickel and J.C. Minx (eds.)]. Cambridge University Press, Cambridge, United Kingdom and New York, NY, USA.
2. PRHYDE. FCH JU project protocol for heavy-duty hydrogen refuelling 2020-2021. https://prhyde.eu/progress/
3. SAE J2601. Fueling protocols for Light duty gaseous hydrogen surface vehicles. https://www.sae.org/standards/content/j2601_201612/).
4. HyTransfer. Pre-normative research on gaseous hydrogen transfer. FCH JU; 2012. 1-325277, https://www.hytransfer.eu/
5. Johnson T, Bozinoski R, Ye J, Sartor G, Zheng J and Yang J. Thermal model development and validation for rapid filling of high pressure hydrogen tanks. Int J Hydrogen Energy 2015;40:9803-14.
6. Galassi M. C, Papanikolaou E, Heitsch M, Baraldi D, Acosta Iborra B and Moretto P. Assessment of CFD models for hydrogen fast filling simulations. Int J Hydrogen Energy 2014;39:6252-60
7. Bourgeois T, Brachmann T, Barth F, Ammouri F, Baraldi D, Melideo D, Acosta-Iborra B, Zaepffel D, Saury D, and Lemonnier D. 2017. Optimization of hydrogen vehicle refuelling requirements. International Journal of Hydrogen Energy 42:13789–809
8. Melideo D, Baraldi D. CFD analysis of fast filling strategies for hydrogen tanks and their effects on key-parameters. Int J Hydrogen Energy 2015;40:735-45.
9. Melideo D, Baraldi D, Galassi MC, Ortiz Cebolla R, Acosta Iborra B and Moretto P. CFD model performance benchmark of fast filling simulations of hydrogen tanks with pre-cooling. Int J Hydrogen Energy 2014;39:4389-95
10. Bourgeois T, Ammouri F, Weber M, Knapik C. Evaluating the temperature inside a tank during a filling with highly-pressurized gas. International Journal of Hydrogen Energy 2015;40:11748-55
11. Moran MJ, Shapiro HN, Boettner DD, et al. Fundamentals of Engineering Thermodynamics. John Wiley & Sons, 2010.
12. Kunz O, Wagner W. The GERG-2008 Wide-Range Equation of State for Natural Gases and Other Mixtures: An Expansion of GERG-2004. J Chem Eng Data 2012; 57: 3032–3091.
13. Rathore MM, Kapuno R. Engineering Heat Transfer. Jones & Bartlett Publishers, 2010.
14. Holman J. Heat Transfer. 10th edition. Boston: McGraw-Hill Education, 2009.
15. Monde, M, Woodfield P, Takano T and Kosaka M. 2012. Estimation of temperature change in practical hydrogen pressure tanks being filled at high pressures of 35 and 70 MPa. International Journal of Hydrogen Energy 37:5723-34
16. Monde, M. and Kosaka, M., "Understanding of Thermal Characteristics of Fueling Hydrogen High Pressure Tanks and Governing Parameters," SAE Int. J. Alt. Power. 2(1):61-67, 2013, https://doi.org/10.4271/2013-01-0474